Journal of Mathematics in Industry
a SpringerOpen Journal

RESEARCH Open Access

Research on aircraft route planning optimization problem with multi-constraints and dual-targets

Qianyu Zhang[1,3], Xianfeng Ding[2*], Jingyu Zhou[1] and Yi Nie[2]

*Correspondence: fxxd@163.com
[2]School of Science, Southwest Petroleum University, Chengdu 610500, China
Full list of author information is available at the end of the article

Abstract

As the core technology in the field of aircraft, the route planning has attracted much attention. However, due to the complexity of the structure and performance constraints of the aircraft, the route planning algorithm does not have well universality, so it cannot be used in a complex environment. In the paper, a multi-constraints and dual-targets aircraft route planning model was established for the real-time requirements of space flight, the dynamic changes of flight environment with time, the accuracy requirements of positioning errors in the safety area, and the minimum turning radius constraints. Based on the directed graph and dynamic programming ideas, the model simulation and model validation were carried out with the data of F question in the *"16th Graduate Mathematical Modeling Contest"*. The results showed that the optimal path length obtained in *data set 1* was *124.61 km*, the number of corrections was *11 times*, the solution time was *2.3768 seconds*, the optimal path length obtained in *data set 2* was *110.00 km*, and the number of corrections was *12 times*. The solution time was *0.0168 seconds*. Multi-constraints and dual-targets aircraft route planning model can plan the flight path of the aircraft intuitively and timely, which confirmed the effectiveness of the model.

Keywords: Route planning; Multi-constraints; Dual-targets; Directed graph

1 Introduction

In the flight space, many factors need to be considered to plan a reasonable path for the aircraft according to actual needs, such as the aircraft's own performance, structure, terrain, threat and so on, so that it can obtain an optimal path at a lower risk [1, 2], which is a NP-complete problem [3]. So far, the aircraft's route planning algorithm is still the focus of research [4, 5]. Route planning belongs to the category of path optimization. According to the continuous and dynamic change of environment model, it is divided into global route planning and real-time local route planning. Generally, the planning space is defined as static, and the algorithm research of global route planning is carried out [6]. The main methods are route planning mathematical methods, such as dynamic planning algorithm, route planning intelligent methods [7–10], including article swarm optimization algorithm, simulated annealing algorithm. Route planning geometric methods, specifically

shortest path algorithm. However, these algorithms do not have well universality and cannot be tracked for specific problems [11]. The route planning must be based on the premise of satisfying the constraints. Otherwise, the route planning is only the approximate ideal route under the assumed conditions, and does not have the feasibility [12].

At present, the research on multi-constraints route planning usually uses the objective function weighting to establish the evaluation index of the model, and obtain the optimal route through the algorithm. Since the aircraft usually needs to plan the flight path before performing the mission and determine a series of way-points. It is known that the flying distance of an aircraft is the shortest when it keeps a direct flight between two adjacent way-points, the distance between the selected way-points of the aircraft is relatively long. During the flight, the aircraft needs to be accurately positioned according to the positioning system to ensure that it can reach the destination and complete the flight mission. There are often positioning errors in the positioning process, including horizontal and vertical errors. The aircraft needs to locate the positioning error during the flight correction, when the aircraft reaches the correction point, it can correct the error according to the error correction type of the position. The location of the correctable flight area depends on the terrain, and there is no uniform rule. If the vertical error and the horizontal error can be corrected in time, the aircraft can fly according to the predetermined route, and the error can be corrected by several correction points to reach the destination. However, when the positioning error accumulates to a certain extent, the aircraft will not be able to fly according to the original planned route. At the same time, due to the limitation of the structure and control system, the aircraft cannot turn in time, so it cannot fly according to the original planning path. Therefore, it is of practical significance to plan reasonably the way-points with dynamic characteristics under multiple constraints.

This paper aims to minimize the path of the aircraft during flight and minimize the number of corrections in the correction area. The dual-targets model was established and the corresponding algorithm was given. Based on the idea of dynamic programming, this method embodies the advantages of multi-stage and decision-making process. Combined with the characteristics of graphical ordered search, it is essentially a path planning algorithm based on geometric principle, step generation and multi-targets constraints.

2 Establishment of multi-constraints and dual-targets route planning model

2.1 Problem statement

Assume that the flight area of the aircraft is as shown in Fig. 1. The starting point is point A and the destination is point B. Its route constraints are as follows:

(1) The aircraft needs real-time positioning during space flight, and its positioning error includes vertical error and horizontal error. For every 1 m flight, the vertical error and horizontal error will increase by δ dedicated units. When reaching the ending point, the vertical error and horizontal error should be less than θ units. To simplify the problem, it is assumed that when both the vertical error and the horizontal error are less than θ units, the aircraft can still fly according to the planned path.

(2) The aircraft needs to correct the positioning error during flight. There are some safe positions (correction points) in the flight area that can be used for error correction. When the aircraft reaches the correction point, it can correct the error according to the error correction type of the position. The location of correction of vertical and horizontal errors can be determined according to the terrain before route planning

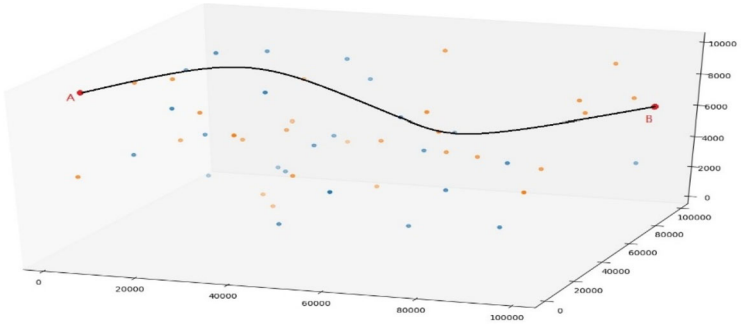

Figure 1 Schematic diagram of the aircraft route planning area

(as shown in Fig. 1, the yellow point is the correction point of horizontal error, the blue point is the correction point of vertical error, the starting point is point A, the destination is point B, and the black curve represents a route). The location of the corrected flight area depends on the terrain and has no uniform rule. If the vertical error and horizontal error can be corrected in time, the aircraft can fly according to the predetermined route, and finally arrive at the destination after error correction through several correction points.

(3) At point A of the departure point, the vertical and horizontal errors of the aircraft are assumed be zero.

(4) After correcting the vertical error of the aircraft at the vertical error correction point, the vertical error will be changed to zero and the horizontal error will remain unchanged.

(5) After the aircraft performs horizontal error correction at the horizontal error correction point, its horizontal error will be changed to zero and the vertical error will remain unchanged.

(6) Assumed that the vertical error of the aircraft is not greater than α_1 units, and the vertical error correction is corrected when the horizontal error is not greater than α_2 units.

(7) Assumed that the vertical error of the aircraft is not greater than β_1 units, and the horizontal error is corrected when the horizontal error is not greater than β_2 units.

(8) The aircraft are limited by the structure and control system during the turn and cannot complete the immediate turn (the direction of the aircraft cannot be changed abruptly), the minimum turning radius of the aircraft is assumed to be 200 m.

Through the above assumptions, the aircraft can finally arrive at the destination after error correction through several correction points.

2.2 Establishment of model

Due to the short distance between way-points relative to the earth, the earth rotation and spherical curvature are ignored. The model of the directional route map and the minimum turning radius arc are established to elaborate framework by considering the least error correction point among the route points, the shortest path length and the minimum turning radius constraints between way-points.

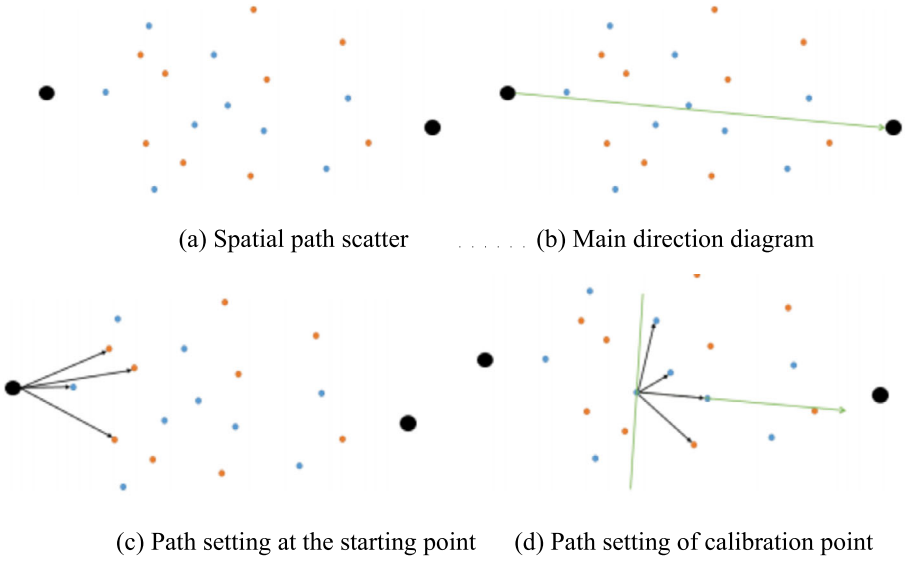

Figure 2 Schematic diagram of the directed graph

2.2.1 Establishment of dynamic directional route map

In the three-dimensional flight space, except for the end point and the start point, there are many correction points, and the correction points are converted into a directional correction point route map by establishing a directed graph, as follows:

(1) Calculated the main direction from the starting point to the ending point;
(2) After an error correction point, the division plane was established by using the principal direction of the point as a normal vector;
(3) Searched all error correction points on the side of the main direction on the segmentation plane (without the ending point);
(4) Assumed that the current horizontal and vertical errors were both zero, all reachable correction points were found according to the constraints;
(5) Add a path from the current point to the reachable point (the direction is the current point points to the reachable point);
(6) Perform the above operations for all points (excluding the ending point).

The establishment diagram of the directional map of the correction point of the spatial error is as follows.

It can be seen from Fig. 2(a) that the original data is randomly scattered in the space to form a spatial undirected scatter point. Figure 2(b) establishes a plane with the normal vector in the main direction from the starting point to the end point, Fig. 2(c) sets the possible path at the starting point, and Fig. 2(d) sets the path at the correction point.

2.2.2 Demonstration of minimum turning radius based on spatial geometry principle

In view of the constraint of the minimum turning radius $R_{\min} = 200$ m, $R \geq 200$ m, it is firstly analyzed and demonstrated in two-dimensional space.

As shown in Fig. 3 and Fig. 4, point $O(0, r)$ is taken as the center of the circle, r as the radius of the circle O, and the tangent of the circle O is taken through the point, and the tangent intersects the circle O at point Q, then point $Q(u_q, v_q)$ meets the following conditions,

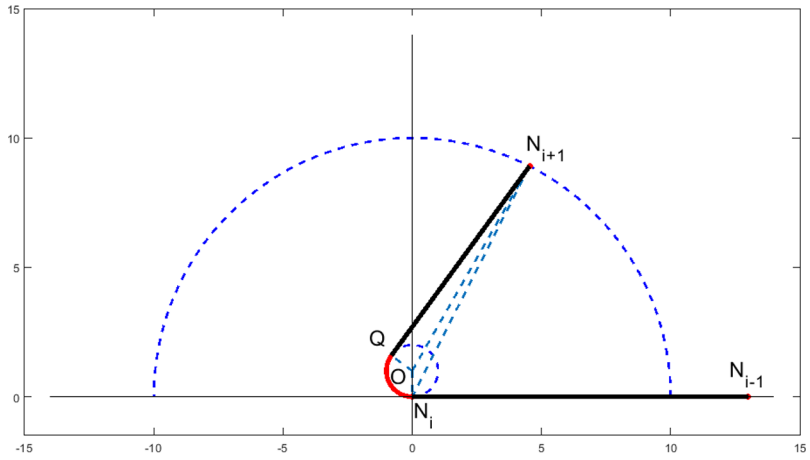

Figure 3 Path analysis of the positive axis in the UV coordinate system

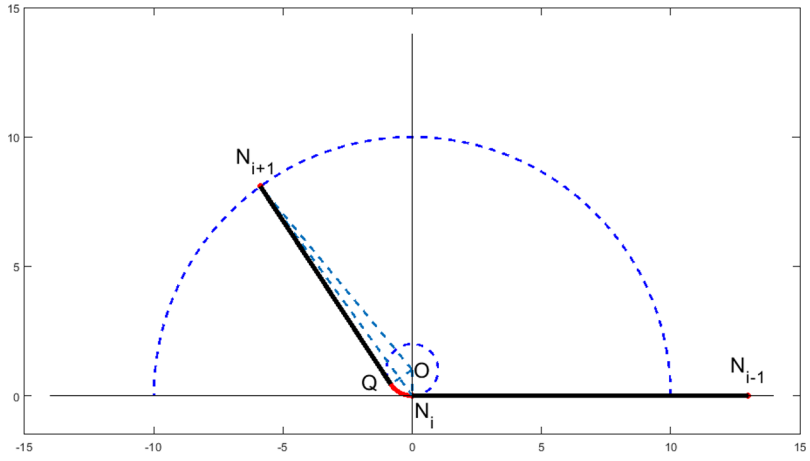

Figure 4 Analysis of the path of the anti-axis direction in the UV coordinate system

(a) Point q is on circle O;
(b) $\overrightarrow{OQ}$ perpendicular to $\overrightarrow{N_{i+1}Q}$;
(c) $N_{i+1}Q$ in the clockwise direction of $\overrightarrow{N_{i+1}Q}$;
The coordinates of Q point are derived as follows,

$$\begin{cases} u_q^2 + (v_q - r)^2 = r^2, \\ u_q(u_q - uN_{i1}) + (u_q - r)(v_q - vN_{i1}) = 0, \\ (u_q - uN_{i1})(vN_{i1} - r) - (v_q - vN_{i1})uN_{i1} > 0. \end{cases} \tag{1}$$

The coordinates of the Q point can be obtained by solving the equations, and the coordinates of the $Q(u_q, v_q)$ point are known. The coordinates of N_{i+1} and N_i are known, and $\overset{\frown}{N_iQ}$ can be obtained. Then you can get the new path:

$$\overset{\frown}{i} = \overset{\frown}{N_iQ} + N_{i+1}Q. \tag{2}$$

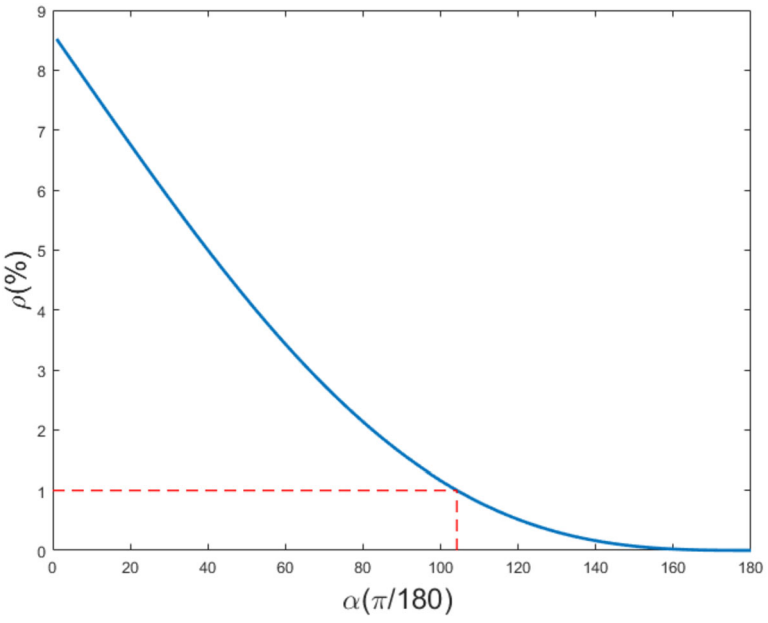

Figure 5 ρ and α changes between the diagram

After repeated calculation and verification, it is found that the complex solution of the coordinates can be transformed into the solution of the route path variation ratio, which simplifies the path solving step and saves computation time. The specific derivation process is as follows:

Let, $\angle N_{i-1}N_iN_{i+1} = \theta_1$, $N_iN_{i+1} = m$, $N_iO = r$; Known $N_i(0,0)$, $O(0,r)$, $N_{i+1}(m\cos\theta_1, m\sin\theta_1)$ and $\overrightarrow{OQ}$ perpendicular to $\overrightarrow{N_{i+1}Q}$, $\overrightarrow{ON_i}$ perpendicular to $\overrightarrow{N_iN_{i+1}}$,

From is, get

$$\overrightarrow{N_{i+1}Q} = \sqrt{|\overrightarrow{N_{i+1}Q}|^2 - |\overrightarrow{OQ}|^2}, \tag{3}$$

and because of $\alpha = \arccos[\frac{\overrightarrow{OQ}\overrightarrow{ON_i}}{|\overrightarrow{OQ}||\overrightarrow{ON_i}|}]$, $\widehat{N_iQ} = r\alpha$, α is the arc system, path is:

$$\widehat{i} = \widehat{N_iQ} + N_{i+1}Q = r\alpha + \sqrt{|\overrightarrow{N_{i+1}Q}|^2 - |\overrightarrow{OQ}|^2}. \tag{4}$$

Then it can be proved that the path change ratio is:

$$\rho = \frac{r\alpha + \sqrt{|\overrightarrow{N_{i+1}Q}|^2 - |\overrightarrow{OQ}|^2} - m}{m}. \tag{5}$$

From Fig. 5, the path variation ratio ρ and α change as follows.

As shown in Fig. 5, the variation ratio ρ gradually decreases as the α increases, and when α is at $[0, 104]$, the change is more severe and shows a downward trend. At that time, the variation ratio ρ is less than 1%, which has little impact on the value of ρ.

From Fig. 6, the variation change ratio ρ and the path length m as follows.

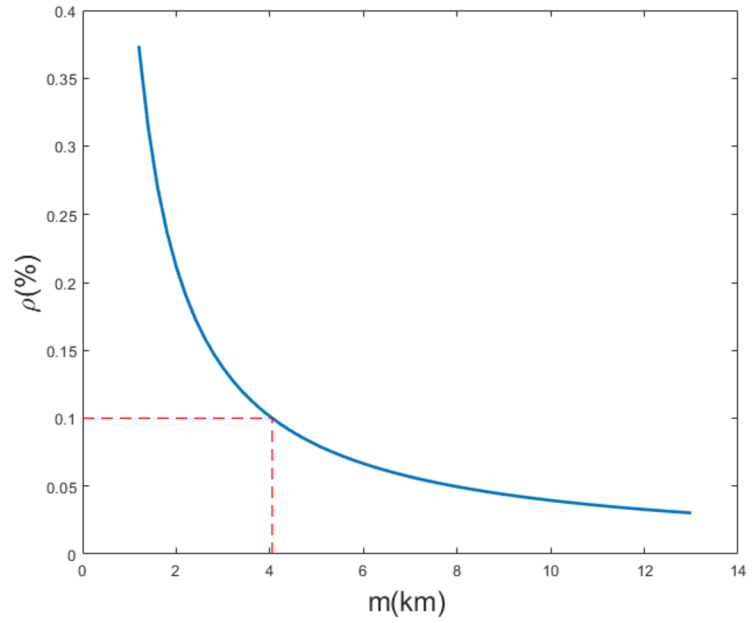

Figure 6 ρ and the path length m change between the diagram

As shown in Fig. 6, The variation ratio ρ gradually decreases as the length m increases. When the length m is greater than 1 km, the variation ratio is less than 1%, and when it is greater than 4.05 km, the change ratio is less than 0.1%, which has little effect on the value of variation ratio ρ.

Through the above analysis, the increase of the calculated route path changes little compared with the optimal route path without the minimum radius is limited.

Since the above inferences are all displayed in the two-dimensional plane coordinate system UV, the two-dimensional plane is now expanded into the three-dimensional space, as shown in Fig. 7.

As shown in Fig. 7, where XYZ represents the coordinate system in three-dimensional space, where N_iN_{i+1}, $\overset{\frown}{N_iO}$, and $N_{i+1}Q$ are the flight paths of the error correction points, the black part is the straight flight path, and the red is the arc flight path.

2.2.3 Establishment of multi-constraints route planning model

It is assumed that the aircraft route planning process has the shortest route length, the least number of corrections, and the minimum turning radius is the objective function, in which the sequence $P = \{\mathrm{A}, N_1, N_2, \ldots N_m, \mathrm{B}\}$ is used to represent the starting point A, the ending point B and the possible correction point.

Minimum turning arc radius model:

$$\overset{\frown}{l} = R\alpha, \tag{6}$$

where R is the turning radius, $\alpha = \arccos[\frac{\overrightarrow{OQ}\overrightarrow{ON_i}}{|\overrightarrow{OQ}||\overrightarrow{ON_i}|}]$.

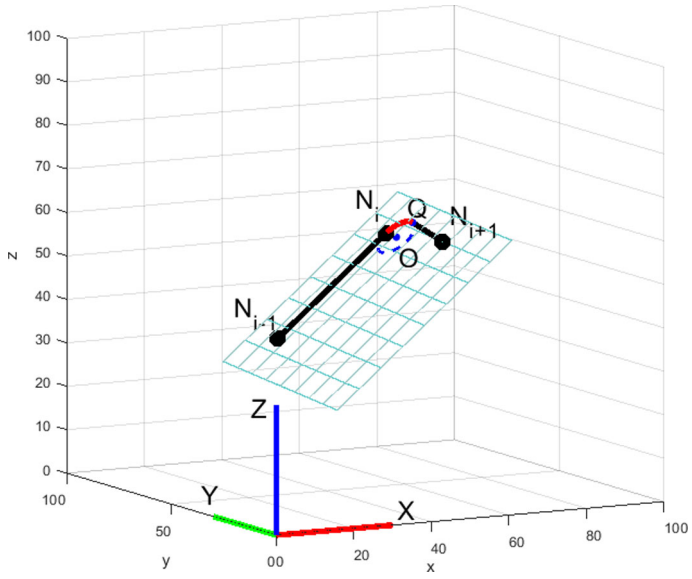

Figure 7 Three-dimensional path analysis diagram

Total route length model:

$$L(P) = \sum_{i=1}^{m} \mathrm{dis}(N_i, N_{i+1}) + \mathrm{dis}(A, N_1) + \mathrm{dis}(N_m, B) + \overset{\frown}{l}\ . \tag{7}$$

Where dis represents the Euclidean distance between two points in space, $\overset{\frown}{l}$ represents minimum turning arc radius.

Model of correction times in route:

$$V(P) = \sum_{i=1}^{m} u_i(x). \tag{8}$$

Where $u_i(x)$ is the number of correction times at ith route node.

$$u_i(x) = \begin{cases} 0, & \text{others}, \\ 1, & \delta h_i(x) < \varphi \text{ or } \delta v_i(x) < \varphi. \end{cases} \tag{9}$$

Where φ is the minimum horizontal and vertical error, $h_i(x)$and $v_i(x)$ are the horizontal and vertical errors of the ith route node. Respectively, when equation $\delta h_i(x) < \varphi$ and $\delta v_i(x) < \varphi$ is satisfied, the correction times of the ith route node shall be recorded as 1, otherwise, the correction times shall be recorded as 0.

Multi-constraints and dual-targets path planning model:

$$\min\left[L(P), V(P)\right]$$

$$\text{s.t.} \begin{cases} \sum_{i=1}^{m-1} h_i(x) < \theta, \\ \sum_{i=1}^{m-1} v_i(x) < \theta, \\ \delta h_i(x) < \varphi, \\ \delta v_i(x) < \varphi, \\ r \geq 200, \\ L_i > L_{\min}. \end{cases} \tag{10}$$

Where $h_i(x)$ and $v_i(x)$ are the horizontal and vertical errors of the ith route node respectively, and $L_{\min}$ is the minimum flight distance between two adjacent correction points.

2.2.4 Model solution based on directed graph and dynamic programming

The introduction of the model running environment is shown in the Table 1.

Algorithm flow chart of route planning model is as follows in Fig. 8.

The specific solution algorithm steps are as follows.

Table 1 Environment introduction

Attributes	Parameter
Processor	Intel(R) Core(TM) i7-7700HQ @ 2.80 GHz
Operating System	Based on x64 processors
System Type	Windows 10
Platform	MATLAN V2018a

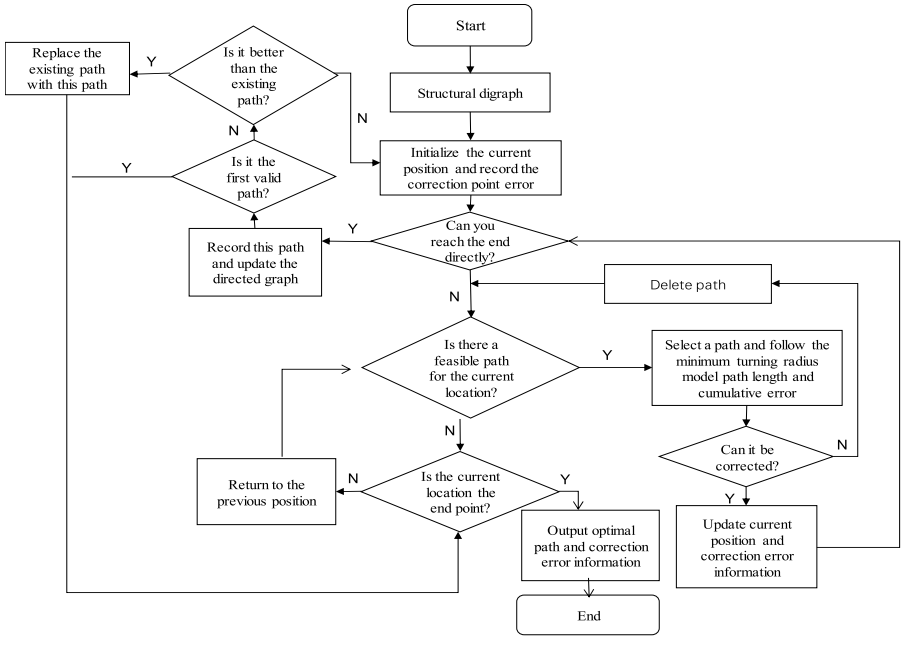

Figure 8 Algorithm flow chart of route planning model

Step1: Construct a route map of the directed correction point according to the distribution of the correction points (including the start point and the end point) in the space;

Step2: Initialize the current position and record the error of the correction point;

Step3: According to the constraint condition to determine whether the path can reach the ending point, if it can, then go to *step 4*, if not, then perform *Step 6*;

Step4: Record the path, and update the directed route map to determine whether the path is the first valid path, if otherwise, execute *Step 5*, if yes, execute *Step 9*;

Step5: Judge whether the path is better than the existing path, if yes, replace the existing path with the path and execute *Step 9*, if otherwise, execute *Step 2*;

Step 6: Judge whether there is a feasible path at the current location. If there is, execute *Step 7*. If not, execute *Step 9*;

Step7: Select a path, calculate the path length and the cumulative error of the correction point according to the minimum turning radius model, and judge whether it can be corrected according to the correction type of the point. If yes, execute *Step 8*. If not, delete the path and return to *Step 6*;

Step 8: Update the current position and correct the accumulated error according to the correction type of the point, and turn to *Step 3*;

Step 9: Judge whether the current point is the ending point. If yes, terminate the algorithm. Otherwise, update the current position to the previous position and turn to *Step 6*.

3 Model application and evaluation

3.1 Model application

In order to verify the feasibility and effectiveness of the algorithm, a simulation experiment was carried out. The verification is performed by using two data sets, wherein the number of correction points in the data set 1 is 613, and the number of correction points in the data set 2 is 317, And each correction point contains coordinate information in space, correction point type, and mark type. The calibration points in the data set 1 are randomly selected as shown in Table 2.

Suppose the parameters in data set 1 are as follows: $\alpha_1 = 25$, $\alpha_2 = 15$, $\beta_1 = 20$, $\beta_2 = 25$, $\theta = 30$, $\delta = 0.001$. The parameters in data set 2 are as follows: $\alpha_1 = 20$, $\alpha_2 = 10$, $\beta_1 = 15$, $\beta_2 = 20$, $\theta = 20$, $\delta = 0.001$.

The solution path planning in data set 1 is shown in Fig. 9.

As shown in Fig. 9, except for the starting point, all the correction points and ending points in the three-dimensional graph include the accumulation of vertical correction error and horizontal correction error, and the correction points are marked in yellow. The starting point and the ending point are marked in red, and the route direction was from left to right. The route length in data set 1 was calculated to be *112.43 km*, and the number of correction are *8 times*. Because of the arc in the route path, it is clearly marked with a

Table 2 Position and correction type of 5 randomly selected points

Calibration point number	*X* coordinate /m	*Y* coordinate /m	*Z* coordinate /m	Calibration point type
0	0.00	50,000.00	5000.00	A
1	33,070.83	2789.48	5163.52	0
2	54,832.89	49,179.22	1448.30	1
3	77,991.55	63,982.18	5945.82	0
4	16,937.18	84,714.34	5360.29	0

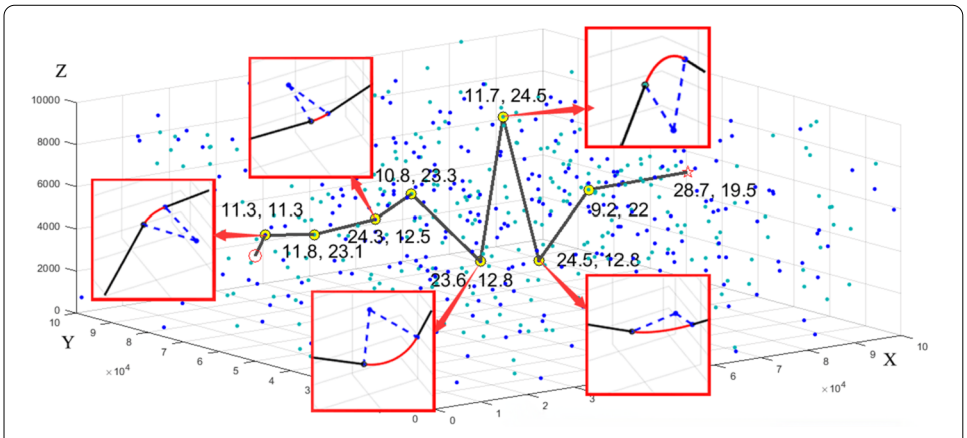

Figure 9 Spatial route planning representation in data set 1

Table 3 Data set 1 route planning table

Calibration point number	Vertical error before correction / unit	Horizontal error before correction / unit	Calibration point type
0	0.00	0	A
346	11.25759118	11.25759118	11
69	11.81499439	23.07258557	01
237	24.31447751	12.49948312	11
233	10.8239642	23.32344731	01
375	23.63017415	12.80620995	11
315	11.69584636	24.50205632	01
406	24.50788624	12.81203988	11
248	9.205034064	22.01707394	01
612	28.71848498	19.51345092	B

red marking box in the figure, and the red arc is the increased path length. The specific route planning table is as follows,

It can be seen from the Table 3 that in addition to the starting point and the ending point, though *8* correction points, the final cumulative vertical error is *28.718 units*, and the horizontal error accumulation is *19.513 units*. Correction point type of 01 indicates that the vertical error correction is successful, correction point type of 11 indicates that the horizontal error correction is successful.

The solution path planning in data set 2 is shown in Fig. 10.

The mark in the Fig. 10 is consistent with Fig. 9. The route length in data set 2 is calculated to be *110.20 km*, and the number of corrections to go through is *12 times*. Because of the arc in the route path, it is clearly marked with a red marking box in the figure, and the red arc is the increased path length. The specific route planning table is as follows,

It can be seen from the Table 4 that in addition to the starting point and the ending point, though 13 correction points, the final cumulative vertical error is *6.960 units*, and the horizontal error accumulation is *13.514 units*. Correction point type of 01 indicates that the vertical error correction is successful, correction point type of 11 indicates that the horizontal error correction is successful.

3.2 Model evaluation

(1) Discussion on the complexity of time and space

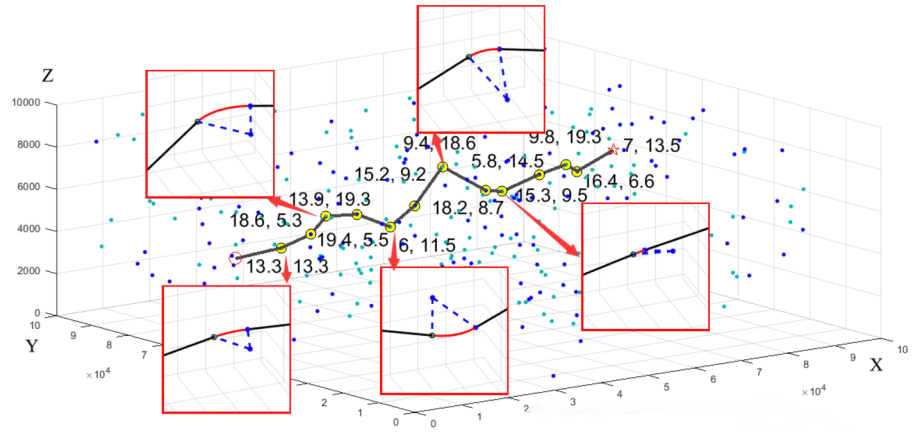

Figure 10 Spatial route planning representation in data set 2

Table 4 Data set 2 route planning table

Calibration point number	Vertical error before correction / unit	Horizontal error before correction / unit	Calibration point type
0	0.00	0	A
163	13.28789761	13.28789761	01
114	18.62205093	5.334153324	11
8	13.92198578	19.2561391	01
309	19.44631118	5.524325401	11
305	5.968714547	11.49303995	01
123	15.17310764	9.204393096	11
231	9.436726707	18.6411198	01
160	18.15390257	8.717175866	11
92	5.776163625	14.49333949	01
93	15.26088202	9.484718396	11
61	9.834209702	19.3189281	01
292	16.38812359	6.553913884	11
326	6.960509275	13.51442316	B

The model established by this algorithm was the nearest point search by KD-tree, which greatly improved the search speed. However, due to the different performance of different data sets in the route space, the position of the correction points was inconsistent, and the calibration point route map was also different, and the time complexity could not be directly calculated. In this paper, we used the method of average value to get the relationship between the data scale n and the calculation time. According to the density of the data correction point distribution, we randomly generated 50 groups of test models for each value of n, and the results are as follows.

It can be observed from Fig. 11 that the average running time increases as the data size n increases.

At the same time, this algorithm used queue to save the current path points to be processed, which greatly reduces the memory consumption of the algorithm itself.

(2) Comparison of time and iteration number

Table 5 shows the length of time spent by the model in two data sets and the number of model iterators.

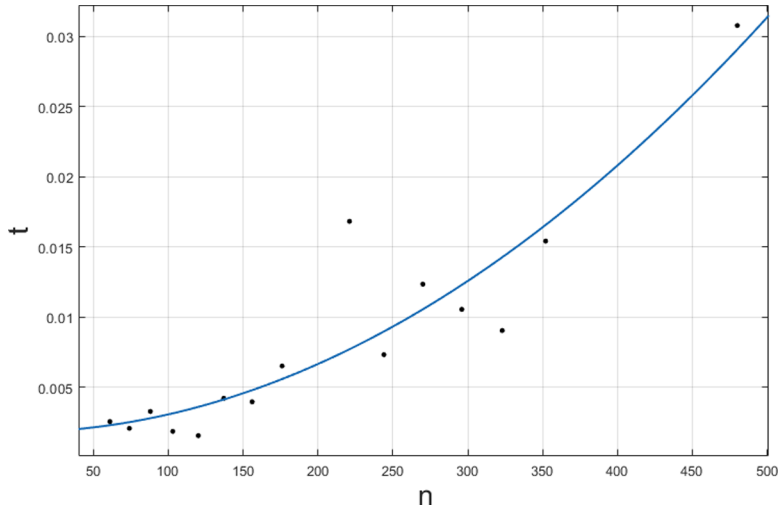

Figure 11 Quantity- time curve graph

Table 5 Comparison of time and iterations

Dataset type	Take times/s	iterator times/s
Dataset 1	2.3769	26,025
Dataset 2	0.0370	207

Through the analysis of the Table 5 and the comparison between data set 1 and data set 2, it is found that the operation results are affected by the number of correction points and correction types in data set 1, which lead to the long time spent in data set 1.

4 Conclusion

In the paper, the real-time requirements of the aircraft in space flight, the dynamic changes of the flight environment with time, the accuracy requirements of the positioning error in the safety area, and the minimum turning radius constraints were fully considered, and finally, the multi-constrained and dual-target aircraft route planning model was established. Through the working principle of pulley block to solve the problem of minimum turning radius restriction, the path scheme was designed and proved by space geometry transformation, which simplified the minimum turning radius restriction. It solved the problem that the positioning system could not accurately located itself due to the structural constraints of the aircraft system, and due to the limitation of structure and control system, the aircraft could not complete the real-time turning. And then, the optimal path was obtained, and the validity and superiority of the model establishment were demonstrated from multiple dimensions. Finally, two kinds of data sets were used to test the model, and the schematic diagram of flight path optimization under the two data sets was drawn, and the optimal path length and the minimum number of aircraft correction were obtained.

Experiments showed that the model established by the algorithm can not only obtain the optimal path, but also the minimum correction point. The optimal path length obtained in *data set 1* is *124.61 km*, the number of corrections is *11 times*, and the optimal result is obtained in *data set 2*. The path length is *110.00 km* and the number of corrections

is *12 times*, and the space complexity and time complexity of the algorithm show good performance.

Supplementary information

Supplementary information accompanies this paper at https://doi.org/10.1186/s13362-020-00094-0.

Additional file 1. Supplementary information (ZIP 80 kB)
Additional file 2. Supplementary information (ZIP 84 kB)

Acknowledgements
Thank you for the data support of the "16th graduate mathematics modeling competition".

Funding
Not applicable.

Abbreviations
NP-complete problem, NP is the problem of Non-deterministic Polynomial, which is the non-deterministic problem of the complexity of polynomial. And if any NP problem can be converted to an NP problem by a polynomial time algorithm, then the NP problem is called the Non-deterministic Polynomial complete problem. NP complete problem is also called NPC problem [13]. NP is the problem of Non-deterministic Polynomial, which is the non-deterministic problem of the complexity of polynomial. And if any NP problem can be converted to an NP problem by a polynomial time algorithm, then the NP problem is called the Non-deterministic Polynomial complete problem. NP complete problem is also called NPC problem [13].; KD-tree, Be known as k-dimensional tree, it is a data structure that divides a k-dimensional data space. It is mainly used for the search of key data in multi-dimensional space (such as range search and nearest neighbor search). KD-tree is a special case of binary space segmentation tree [14]..

Availability of data and materials
The data sets supporting the results of this article are included within the article and its additional files. Additional file 1 contains raw data for dataset 1 and dataset 2. Additional file 2 contains result data for dataset 1 and dataset 2.

Competing interests
The authors declare that they have no competing interests.

Authors' contributions
QZ responsible for experiment design, experiment analysis and article writing; XD responsible for the overall thought arrangement; JZ responsible for experiment analysis and code writing; YN responsible for mathematical model building and analysis data. All authors read and approved the final manuscript.

Author details
[1]School of Computer Science, Southwest Petroleum University, Chengdu 610500, China. [2]School of Science, Southwest Petroleum University, Chengdu 610500, China. [3]*Present address:* School of Information and Electronics, Beijing Institute of Technology, BeiJing 100081, China.

Publisher's Note

Received: 18 November 2019 Accepted: 5 October 2020 Published online: 28 October 2020

References

1. Szczerba RJ, Galkowski P, Glicktein IS. Robust algorithm for real-time route planning. IEEE Trans Aerosp Electron Syst. 2000;36(3):869–78.
2. Chakrabarty A, Jack W. Flight path planning for UAV atmospheric energy harvesting using heuristic search. In: AIAA guidance, navigation and control conference. 2010.
3. Chen Q. Research on constrained multi-source and multi-purpose path problem based on genetic algorithm. Xi'an University of Technology. 2006.
4. Zeng J, Shen G. A method for autonomous variable step path planning of unmanned aerial vehicles. J Projectiles Missiles Guidance. 2008;28(6):21–4.
5. Tang Q, Zhang X, Zou L. Preliminary study on the algorithm of UAV route planning. Aviation Comput Technol. 2003;33(1):125–8.
6. Guo Y, Zhu H. Linchen Shen: flight route planning based on genetic algorithm. Computer Simulation. 2004;21(2):69–71.
7. Twigg SS. Optimal path planning for single and multiple aircraft using a reduced order formulation. Georgia Institute of Technology. 2007.
8. Richards N, Sharma M, Ward D. A hybrid A*/Automaton approach to on-line path planning with obstacle avoidance. In: Proceedings of the AIAA intelligent systems technical conference. 2004.

9. Mitsutak K, Higashino SI. A DP-EC path-planning method for UAVs considering required time range of arrival. In: AIAA guidance, navigation and control conference. 2013.
10. Geiger B, Horn J, Delullo A. Optimal path planning of UAVs using direct collocation with nonlinear programming. 2013.
11. Zhou C, Yan L, Tan Y. Real-time operational strategies for truckload pickup and delivery problems. In: Proceedings of the IEEE international conference on cognitive informatics. 2007.
12. Xiong DJ, Cai SC, Liu YK. Aircraft route planning under multiple constraints. J Projectiles Arrows Guidance. 2009;29(2):289–92.
13. Review HRL, Garey MR, Johnson DS. Computers and intractability. A guide to the theory of NP-completeness. J Symb Log. 1983;48(2):498–500.
14. Adams A, Gelfand N, Dolson J. Gaussian KD-trees for fast high-dimensional filtering. ACM Trans Graph. 2009;28(3):21.